This article has been accepted for publication in a future issue of this journal, but has not been fully edited. Content may change prior to final publication. Citation information: DOI 10.1109/TPWRD.2015.2507541, IEEE Transactions on Power Delivery

Distribution Systems High Impedance Fault Location: a Parameter Estimation Approach

Leonardo U. Iurinic *Student Member IEEE*, A. R. Herrera-Orozco, Renato G. Ferraz, *Member IEEE*, Arturo S. Bretas, *Senior Member IEEE*

***Abstract*—High impedance fault location has always been a challenge for protection engineering. On the other hand, if this task is successfully realized maintenance action could be performed in order to avoid potential injuries. For an effective protection scheme the high impedance fault location should be performed, but a lack of research on this area is noted. This paper proposes a new analytical formulation for high impedance fault location in power systems. The approach is developed in time domain, considering a high impedance fault model composed by two antiparallel diodes. Using this model, the fault distance and parameters are estimated as a minimization problem. Firstly, a linear least square based estimator is applied without consideration of line capacitance. Secondly, a steepest descent based estimator is proposed in order to consider the line capacitance. Studies were carried out with the IEEE 13 bus modeled in ATP. Encouraging test results are found indicating the method's potential for real life applications.**

***Index Terms*— High Impedance Fault, Fault Location,**

A particular and worrisome case of power systems faults are the High Impedance Faults (HIF). These faults are usually caused by an unwanted contact of a bare-energized conductor with a surface that significantly restricts the flow of fault current to a level below the detectable by conventional overcurrent devices [1]. The most common causes of such faults in Power Distribution Systems (PDS) are broken conductors contact with poorly grounded objects, like trees, vehicles and wood fences. A HIF does not behave as a linear resistance, as classical fault location methods assume, instead it tends to present a nonlinear behavior of voltage as a function of current due to existence of electric arcs and modification in surface conditions [2].

At this point, it is important to refer to the non-permanent arcing faults, whose features are close to those of HIF [3], [4]. Arcing faults also maintain a nonlinear characteristic between voltage and current, but producing detectable fault current levels. Thus, solutions given for the detection and location of arcing faults could contribute in solving the issues concerned with the HIF. Contrary to HIF, arcing faults tends to be self-cleared by the automatic switchgear action [4], [5]. Hence, arcing faults detection and location must be done in a short window of time, a limitation that is not applied to HIF detection and location.

The detection of HIF and arcing faults presents great challenges. Many works have been realized in this subject, as [3], [6]–[11]. For this purpose, the estimation of the fault location is the next natural step after detection. Conversely, comparatively less research studies have been conducted to estimate the HIF location.

In a broad sense, some basic research lines can be identified in the technical literature. The first consists on simultaneous HIF detection and faulted point direction estimation [8]–[10]. This approach requires for accurate fault location directional-detection devices installed and synchronized on the power network. Other approaches try to estimate the fault location using remote power system measurements. These works proposed to use knowledge-based techniques to solve the HIF impedance and high frequency based fault location approach [14]. This approach shown good results but has not been tested for HIF cases.

Analyzing the technical literature, none of the approaches presented for HIF location can be defined as best, rather which, each one complements the other and their implementation depends on the available resources. On the other hand, currently a lack of consistent mathematical formulations for HIF location is perceived, mainly because a HIF model is not included in the equation derivation. In this context, the present work develops a formulation for fault location that includes a HIF model [2]. The final result can be classified as a contribution for the directional-detection approach with emphasis in primary distribution systems, providing fault distance estimation for detected HIF. For this purpose, studies as [3]–[5], [7] have been taken as primordial references. Still, in comparison with previous works, the proposed approach considers a more complete HIF model, line capacitance and equation derivation is made in phase-components, allowing the consideration of unbalanced operation.

The remainder of this paper is as follows. Section II describes the proposed analytical methodology. Section III describes methodology implementation aspects. A case study is presented on Section IV. Section V presents the conclusions of this work.

L. U. Iurinic and A. R. Herrera-Orozco are with the *Universidade Federal do Rio Grande do Sul*, Porto Alegre RS 90035-190, Brazil (e-mail: uiurinic@ece.ufrgs.br, ricardo.herrera@ufrgs.br).

R. G. Ferraz is with the *Universidade de Caxias do Sul*, Caxias do Sul RS 95070-560, Brazil (e-mail: rgferraz@ucs.br).

A. S. Bretas is with the *University of Florida*, Gainesville, FL 32611-6200, USA (e-mail: arturo@ece.ufl.edu).

This article has been accepted for publication in a future issue of this journal, but has not been fully edited. Content may change prior to final publication. Citation information: DOI 10.1109/TPWRD.2015.2507541, IEEE Transactions on Power Delivery

II. Estimation of Fault Parameters Together with the Fault Distance

The HIF model proposed by [2] or the one presented in [15] can be represented by a mathematical model similar to the arcing fault model of [5] or [7]. In this context, the use of a Least Square Estimation (LSE) approach to estimate the HIF parameters together with the fault distance is proposed. Consider the single-phase line system illustrated in Fig. 1. This is a radial system fed at node 1. Upstream system from node 1 is modeled by a Thévenin source and its equivalent impedance. An equivalent load at node 2 represents the downstream system. Still, a phase to ground fault at point F is considered. The line model considered between node 1 and the faulted point is illustrated in the same figure, where *R*, *L* and *C* represent the per-unit-length line resistance, inductance and shunt capacitance. To simplify the analysis it is assumed that all the capacitance of the line is concentrated at node 1. All equations are initially developed for the single-phase line model. After, they will be extended for a three-phase system, considering single-phase to ground faults. In this work, the phase domain representation is chosen instead of the symmetrical components one. This selection aims formulation generalization, as it allows unbalanced system operation consideration.

Bearing in mind the faulted line model of Fig. 1 and that voltage and current samples are measured at terminal 1, an expression that relates the measured quantities as a function of

$$v_1 = x\left(R i_{1F} + L i'_{1F}\right) + v_F. \quad (1)$$

In (1), x is the fault distance, i_{1F} is the current that flows to the fault through the series branch of the line model and v_F is the fault voltage. An apostrophe is used to indicate the first derivative in function of time and two apostrophes indicate the second derivative. In order to express (1) as a function of the measured current at terminal 1, the effect of the shunt capacitance must be considered:

$$i_{1F} = i_1 - xCv'_1. \quad (2)$$

Finally, replacing (2) into (1), an equation that relates the measured voltage and current at node 1 with the fault distance and line parameters can be derived:

$$v_1 = xR\left(i_1 - xCv'_1\right) + xL\left(i'_1 - xCv''_1\right) + v_F. \quad (3)$$

Line parameters can be calculated from the line topology or can be estimated by means of measurements [16], but the voltage at point F is also needed and it is not straightforward to obtain. If both voltage and current measurements at terminal 2 are available, v_F can be estimated by an equation similar to (3) [17]. On the other hand, the estimation of v_F can be made indirectly by means of a fault model. In traditional one-terminal fault location methods this model consists on a linear resistor connected to ground or between faulted phases [18]. Although this assumption is widely accepted in the research community, it will produce unacceptable results if a HIF case is analyzed. For this reason, a HIF model must replace the classical linear resistor model in order to develop an adequate mathematical approach for fault location. Therefore, the anti-parallel HIF model illustrated in Fig. 2, proposed by [2] and analysed in [15] is considered. Such model yields currents and voltage-current characteristics that are similar to field test results. This can be seen when voltage and current waveforms generated by the model of Fig. 2 are compared with those presented in [17] or [18]. This model consideration provides a path to solve equation (3), aiming fault distance and parameters estimation.

Considering the HIF model illustrated in Fig. 2, the fault voltage can be expressed as a function of the fault current:

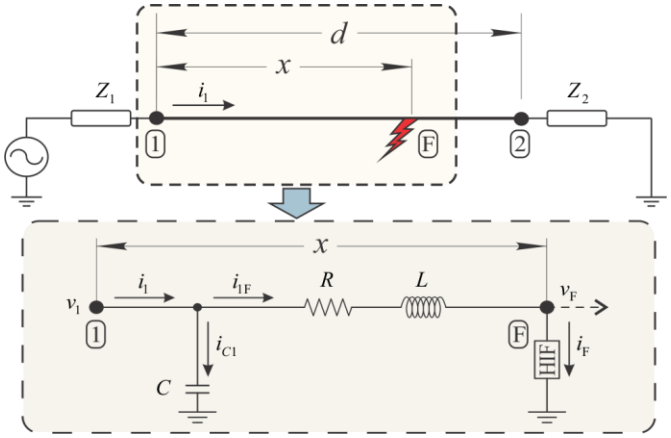

Fig. 1. Single-phase two-terminal line model and a fault at point F.

present when i_F is in its positive semi-cycle and, V_{Fn} is the negative arc voltage, present when i_F is in its negative semi-cycle. These two arcing voltages sources cannot exist at the same moment, and they are turned on and turned off using the following functions:

$$\mathrm{sgp}\left(i_F\right) = \begin{cases} 1, & i_F > 0 \\ 0, & i_F \le 0 \end{cases}. \quad (5)$$

$$\mathrm{sgn}\left(i_F\right) = \begin{cases} 0, & i_F \ge 0 \\ -1, & i_F < 0 \end{cases}. \quad (6)$$

By the replacement of (4) into (3), the fault voltage is embedded in the HIF model, and (3) becomes:

$$v_1 = x\left(R i_1 + L i'_1\right) + R_F i_F + L_F i'_F + V_{Fp}\mathrm{sgp}\left(i_F\right) + V_{Fn}\mathrm{sgn}\left(i_F\right) - x^2\left(RCv'_1 + LCv''_1\right). \quad (7)$$

At this point it is essential to highlight that parameters x, R_F, L_F, V_{Fp} and V_{Fn} are considered to remain constant during the analyzed period. In turn, this assumption is not exactly true in the first period after the fault begins, when the buildup

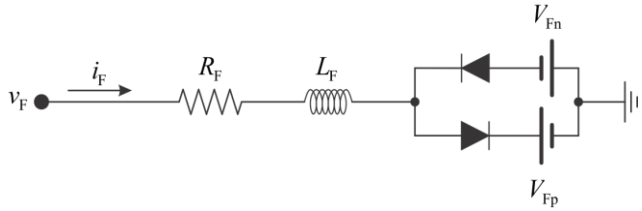

Fig. 2 High Impedance Fault model proposed in [2]

This article has been accepted for publication in a future issue of this journal, but has not been fully edited. Content may change prior to final publication. Citation information: DOI 10.1109/TPWRD.2015.2507541, IEEE Transactions on Power Delivery

phenomenon occurs [20]. However, the shoulder phenomenon is characterized by temporary constant values of the HIF parameters and, after some cycles the fault tends to stabilize. For this reason, the fault parameters are assumed constant in the formulation.

Still, it is possible to rewrite (7) in matrix notation:

$$v_1 = \begin{bmatrix} x & R_F & L_F & V_{Fp} & V_{Fn} & x^2 \end{bmatrix} \cdot \begin{bmatrix} v_s & i_F & i'_F & \mathrm{sgp}(i_F) & \mathrm{sgn}(i_F) & v_{sh} \end{bmatrix}^T, \quad (8)$$

where:

$$v_s = \left(Ri_1 + Li'_1\right); \quad (9)$$

$$v_{sh} = \left(-RCv'_1 - LCv''_1\right). \quad (10)$$

Expression (8) is very elegant but shows two main difficulties to be overcome. The first is the appearance of a quadratic term of the fault distance that leads to a nonlinear relation and, the second drawback is the remaining of the fault current i_F and its derivative. If the line capacitance is neglected, the signal v_{sh} vanishes and the first difficulty is avoided. The disregard of the line capacitance is then considered as a first approximation, leaving to a linear relation in (8) and simplifying its solution. Regarding to the second drawback, there is no simply way to get around this problem, meaning that the fault current must be estimated. In turn, different ways can be conceived in order to estimate i_F and the approach used in this work is explained in section III.

written for a set of N samples and constitute the following system of equations:

$$\begin{bmatrix} v_{1,1} \\ v_{1,2} \\ \vdots \\ v_{1,N} \end{bmatrix} = \begin{bmatrix} v_{s,1} & i_{F,1} & i'_{F,1} & \mathrm{sgp}(i_{F,1}) & \mathrm{sgn}(i_{F,1}) \\ v_{s,2} & i_{F,2} & i'_{F,2} & \mathrm{sgp}(i_{F,2}) & \mathrm{sgn}(i_{F,2}) \\ \vdots & \vdots & \vdots & \vdots & \vdots \\ v_{s,N} & i_{F,N} & i'_{F,N} & \mathrm{sgp}(i_{F,N}) & \mathrm{sgn}(i_{F,N}) \end{bmatrix} \cdot \begin{bmatrix} x \\ R_F \\ L_F \\ V_{Fp} \\ V_{Fn} \end{bmatrix} \quad (11)$$

In order to obtain (11) the transpose of (8) was considered as well as the line capacitance was neglected. In equation (11) numbers after coma indicates the sample number. Still, this relation has a linear system of equations form:

$$\mathbf{y} = \mathbf{X}\hat{\boldsymbol{\theta}} + \xi, \quad (12)$$

where $\mathbf{y}$ is the vector of sampled v_1, $\mathbf{X}$ is the first matrix of (11), called regressors matrix and $\hat{\boldsymbol{\theta}}$ is the estimated vector of parameters. The vector ξ has the same dimension of $\mathbf{y}$ and was added in order to represent the noise.

Clearly (12) has a structure that allows the application of the classical LSE approach for parameter estimation, which consists on the minimization of the quadratic norm of the vector ξ expressed as:

$$J_{\boldsymbol{\theta}} = \xi^T \xi. \quad (13)$$

The final solution of (13) is a simple algebraic relation given by:

$$\hat{\boldsymbol{\theta}} = \left(\mathbf{X}^T\mathbf{X}\right)^{-1}\mathbf{X}^T\mathbf{y}. \quad (14)$$

The solution of (14) is a simple task to achieve with modern digital computation systems. The unique requirement is an adequate selection of samples.

All equations were developed for a single-phase system consideration. However, their extension to a three-phase system is simply done by the replacement of the parameters R, L, C, as well as x, R_F, L_F, V_{Fp} and V_{Fn} by 3x3 matrices and, signals v_1, i_1 and i_F by 3x1 signal vectors. Then, after some straightforward algebra, equation (11) can be extended for three-phase lines as:

$$\begin{bmatrix} \boldsymbol{v}_{1,1}^T \\ \boldsymbol{v}_{1,2}^T \\ \vdots \\ \boldsymbol{v}_{1,N}^T \end{bmatrix} = \begin{bmatrix} \boldsymbol{v}_{s,1}^T & \boldsymbol{i}_{F,1}^T & \boldsymbol{i}_{F,1}^{\prime T} & \mathrm{sgp}\left(\boldsymbol{i}_{F,1}^T\right) & \mathrm{sgn}\left(\boldsymbol{i}_{F,1}^T\right) & \boldsymbol{v}_{sh,1}^T \\ \boldsymbol{v}_{s,2}^T & \boldsymbol{i}_{F,2}^T & \boldsymbol{i}_{F,2}^{\prime T} & \mathrm{sgp}\left(\boldsymbol{i}_{F,2}^T\right) & \mathrm{sgn}\left(\boldsymbol{i}_{F,2}^T\right) & \boldsymbol{v}_{sh,2}^T \\ \vdots & \vdots & \vdots & \vdots & \vdots & \vdots \\ \boldsymbol{v}_{s,N}^T & \boldsymbol{i}_{F,N}^T & \boldsymbol{i}_{F,N}^{\prime T} & \mathrm{sgp}\left(\boldsymbol{i}_{F,N}^T\right) & \mathrm{sgn}\left(\boldsymbol{i}_{F,N}^T\right) & \boldsymbol{v}_{sh,N}^T \end{bmatrix} \cdot \begin{bmatrix} \boldsymbol{x} \\ \mathbf{R}_F \\ \mathbf{L}_F \\ \mathbf{V}_{Fp} \\ \mathbf{V}_{Fn} \\ \boldsymbol{x}^2 \end{bmatrix} \quad (15)$$

Note that all variables in (15) are in bold indicating that they are matrices.

$$\boldsymbol{v}_1 = \begin{bmatrix} v_{1a} & v_{1b} & v_{1c} \end{bmatrix}^T, \quad (16)$$

$$\boldsymbol{i}_1 = \begin{bmatrix} i_{1a} & i_{1b} & i_{1c} \end{bmatrix}^T, \quad (17)$$

$$\boldsymbol{i}_F = \begin{bmatrix} i_{Fa} & i_{Fb} & i_{Fc} \end{bmatrix}^T, \quad (18)$$

$$\begin{bmatrix} & & \end{bmatrix}^T \quad (19)$$

$$\mathbf{R}_F = \begin{bmatrix} R_{Fa} & 0 & 0 \\ 0 & R_{Fb} & 0 \\ 0 & 0 & R_{Fc} \end{bmatrix}, \quad (21)$$

$$\mathbf{L}_F = \begin{bmatrix} L_{Fa} & 0 & 0 \\ 0 & L_{Fb} & 0 \\ 0 & 0 & L_{Fc} \end{bmatrix}, \quad (22)$$

$$\mathbf{V}_{Fp} = \begin{bmatrix} V_{Fpa} & 0 & 0 \\ 0 & V_{Fpb} & 0 \\ 0 & 0 & V_{Fpc} \end{bmatrix}, \quad (23)$$

$$\mathbf{V}_{Fn} = \begin{bmatrix} V_{Fna} & 0 & 0 \\ 0 & V_{Fnb} & 0 \\ 0 & 0 & V_{Fnc} \end{bmatrix} \quad (24)$$

and

$$\boldsymbol{x} = \begin{bmatrix} x & 0 & 0 \\ 0 & x & 0 \\ 0 & 0 & x \end{bmatrix}. \quad (25)$$

Signals (19) and (20) are calculated respectively with (9) and (10), considering the line series resistance and inductance matrices and the shunt capacitance matrix.

The equations (11) or (15) can also be valid for a section downstream node 2 of Fig. 1. Thus, if a section has a mixed

This article has been accepted for publication in a future issue of this journal, but has not been fully edited. Content may change prior to final publication. Citation information: DOI 10.1109/TPWRD.2015.2507541, IEEE Transactions on Power Delivery

distribution line type, as a mixed overhead line and cable, the section should be divided into the necessary number of single distribution line types. Downstream line sections are analyzed if estimated fault location is higher than section length. In order to apply the formulation on downstream line sections, initial line section node voltages and currents are necessary. Current and voltage signals should be propagated to the next node using equation (3).

III. Implementation of the Proposed Approach

In the previous section the theoretical development of the formulation was presented without considering computational implementation issues. Aspects related with fault current estimation, numerical signal derivatives calculation and the choice of samples to apply the LSE are described in this section.

A. Fault current estimation

The primordial difficulty with one-terminal fault location formulations is the need to estimate the fault current. In order to provide a mathematical path for fault current estimation, the superposition theorem is considered. Consider the circuit represented in the Fig. 1. At the fault period, the current leaving node 1 is composed by the load current, line capacitance current and the fault current. As a HIF produces a low current in comparison with the load current, one can assume that the load current is not significantly modified by ground faults, it makes sense to use the difference between the fault and pre-fault residual currents as an estimation of the fault current, similar to the proposed by [4]. However, as considered signals in this work are in time domain, the subtraction must be made from the corresponding samples of different cycles. We propose the implementation of such by a cycle-by-cycle difference digital filter as illustrated in Fig. 3. Samples subtraction using three cycles before the actual fault instant shown to provide an accurate estimation and was in this work applied.

B. Numerical derivatives

The need of the first and second signal derivatives knowledge in the proposed formulation makes necessary the selection of an estimation method. Thus, several numerical derivative approaches were studied. The selected method consisted on the polynomial approximation approach [21]. This method models the signal through a polynomial formulation. Estimation of polynomial coefficients are realized considering a small sample window and applying the least square estimation method [21]. After, the analytical derivative of the estimated function is used to approximate the analyzed signal derivative.

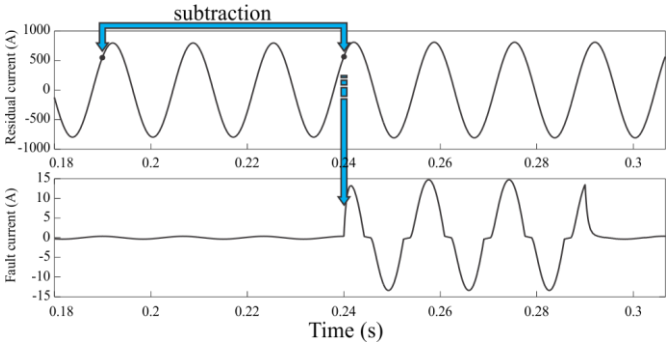

Fig. 3. Illustration of the fault current estimation.

Thus, the digital signal is approximated using a short time window by:

$$y(n) = \alpha_0 + \alpha_1 n + \ldots + \alpha_{k-1} n^{k-1} + \alpha_k n^k + e(n),\ n_i \le n \le n_f . \quad (26)$$

Where k is the polynomial degree, $e(n)$ is the regression error, and n_i, n_f the index corresponding to the beginning and the end of the interval of samples where the approximation is being calculated. Therefore, in this window the following matrix relation can be written:

$$\begin{bmatrix} y(n_i) \\ \vdots \\ y(n_f) \end{bmatrix} = \begin{bmatrix} 1 & n_i & \cdots & n_i^{k-1} & n_i^k \\ \vdots & \vdots & \cdots & \vdots & \vdots \\ 1 & n_2 & \cdots & n_f^{k-1} & n_f^k \end{bmatrix} \begin{bmatrix} \alpha_0 \\ \alpha_1 \\ \vdots \\ \alpha_{k-1} \\ \alpha_k \end{bmatrix} + \mathbf{e} \quad (27)$$

$$\mathbf{y} = \mathbf{X}\hat{\boldsymbol{\theta}} + \mathbf{e} \quad (28)$$

Therefore, parameters $\hat{\boldsymbol{\theta}}$ of (28) can be estimated using

obtained by:

$$\hat{y}'(n_0) = \hat{\alpha}_1 + \ldots + (k-1)\alpha_{k-1} n_0^{k-2} + k\,\alpha_k n_0^{k-1}, \quad (29)$$

$$\hat{y}''(n_0) = \hat{\alpha}_2 + \ldots + (k-2)(k-1)\alpha_{k-1} n_0^{k-3} + (k-1)\alpha_k n_0^{k-2}. \quad (30)$$

The maximum order of the derivative that can be estimated using this methodology is limited to the degree k of the estimated polynomial. In addition, the minimum number of samples that must be considered is k+1. In this work, the signals were approximated with third-degree polynomials using eleven samples per window [21]. The reference sample is located at the middle of the estimation windows.

C. Implementation of the Least Square Estimation

Equation (11) shows that positive and negative parts of the fault current must be used in order to apply the LSE approach. If only a negative or positive semi-cycle of i_F is considered, the fourth or fifth column of the regressors matrix **X** will be zero and then the matrix becomes singular. Therefore, in this case one of these columns must be excluded from the equation and, the same can said about equation (15). If the selected window contains both positive and negative semi-cycles of the fault current, equations (11) and (15) can be directly used.

In order to avoid an extensive study of best set of samples to solve the LSE problem selection, equation (14) was implemented in a moving window of 1.5 cycle length.

This article has been accepted for publication in a future issue of this journal, but has not been fully edited. Content may change prior to final publication. Citation information: DOI 10.1109/TPWRD.2015.2507541, IEEE Transactions on Power Delivery

Therefore, the LSE is performed for each window as a filter and the results are automatically calculated when an HIF occurs.

Simulation tests presented unsatisfactory results when estimation of the fault current is near its zero crossing. Therefore, a function was programed in order to select the appropriate samples of voltages and currents to apply the LSE algorithm. This function selects the samples corresponding with an estimated fault current that exceeds a predefined threshold. The procedure is initiated with the obtaining of the maximum absolute value of the estimated fault current into a moving window of 1.5 cycle. This value is finally multiplied by an empirical factor of 0.15 in order to get the threshold.

The overall process of the LSE implementation is illustrated in the Fig. 4. J1 is the window where the LSE is applied and J2 is the window where the threshold is obtained. J2 is shifted to the pair of J1 and is applied on the estimated fault current.

D. Solution Considering Line Capacitance

If the line capacitance is considered, the nonlinear relation shown in (15) reflects closer the behavior of the system illustrated in Fig. 1. The assumption of the line capacitance implies that the proposed linear LSE is no longer the correct approach to estimate the HIF parameters and the fault distance. In order to take into account the line capacitance, a suitable algorithm must be used to solve the nonlinear relation presented in (15). The selected approach used in this work was obtained with the residue function (15) and the steepest descent Newton's method [22]. This is a nonlinear LSE approach (NLLSE), applied with the samples between 0.5 and 2.5 cycles after fault inception. The threshold used is an average of the linear LSE based method threshold.

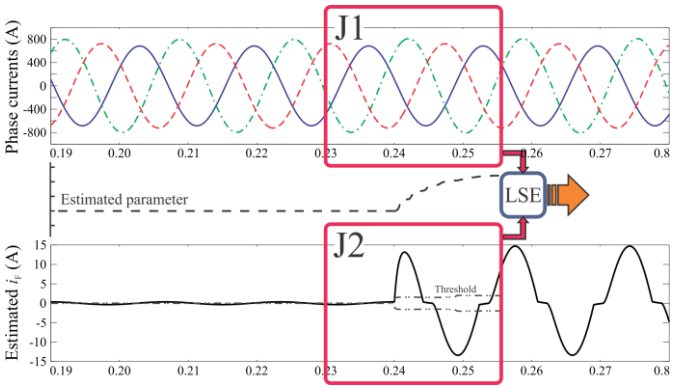

Fig. 4. Implementation of the linear least squares estimation approach for fault location.

IV. Proposed Validation Test

In order to validate the proposed formulation, several HIF were simulated on the modified IEEE 13 nodes test feeder illustrated in the Fig. 5 [23]. This figure shows a Disturbance Monitoring Equipment (DME) at the substation, indicating that voltage and current waveforms are acquired at this location. Dashed line arrows indicate that others DME could also be installed in different branches of the distribution system, establishing a distributed measurement configuration that can be used to improve the fault location. It should be clear however that the proposed methodology does not require such remote measurements. Modifications made on the IEEE 13 nodes test feeder were: the substitution of the voltage regulator at node 650 by a transformer; replacement of the underground cables by overhead lines and all loads were modeled as constant impedance. In order to get an idea of the simulated system load, the RMS currents as phase *a*, *b* and *c* are 484 A, 563.6 A and 515.5 A, respectively.

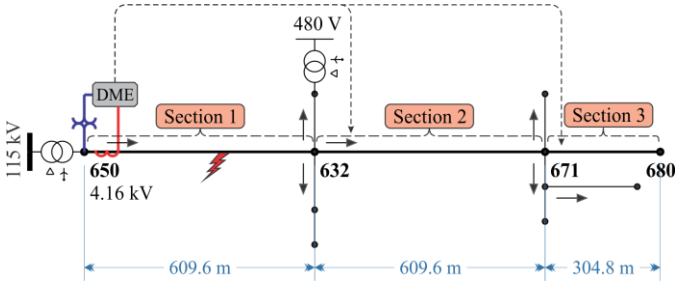

Fig. 5. Diagram of the IEEE 13 nodes test feeder [23]. Principal section is drawn in thick line and is composed by sections 1, 2 and 3.

Only faults on the main section 1 were simulated using the model presented in Fig. 2. Table I presents the parameters used to simulate the HIF. Each combination of parameters was randomly chosen and identified with the number shown in the first column of the Table I. In this table one can see that fault currents are very low with relation to the actual load current inception instants. The time step used in the ATP simulation was of 1 μs and all resulting signals were resampled at a sampling rate of 256 samples per cycle of 60 Hz.

TABLE I
HIGH IMPEDANCE FAULT MODEL PARAMETERS

Id	i_F (%)*	R_F (Ω)	XL_F (Ω)	V_{Fp} (V)	V_{Fn} (V)
1	40.9	10	0	0	0
2	39.1	10	1	80	100
3	6.2	50	10	500	700
4	2.4	100	23	1000	1200
5	1.6	150	30	1000	1200
6	1	200	45	1200	1400
7	1.5	160	26	1110	1100
8	2.4	115	15	800	900
9	2.4	134	21	360	670
10	4.1	80	10	410	600

* Percentage in relation of 563.6 A, the RMS load current at phase *b*.

In the subsequent analyses, the perceptual estimation errors were calculated as:

$$\text{error} = \frac{(\text{estimated fault distance}) - (\text{fault distance})}{(\text{line length})} 100\% \quad (31)$$

for the fault distance and:

$$\text{error} = \frac{(\text{estimated parameter}) - (\text{parameter})}{(\text{parameter})} 100\% \quad (32)$$

for the others parameters. Equations (31) and (32) are not

This article has been accepted for publication in a future issue of this journal, but has not been fully edited. Content may change prior to final publication. Citation information: DOI 10.1109/TPWRD.2015.2507541, IEEE Transactions on Power Delivery

presented as an absolute value error. Therefore a negative error means parameter under-estimation and a positive error means over-estimation.

A. *HIF at section 1: a particular case of the linear LSE*

The first analysis consisted on applying HIF, characteristics presented in TABLE I, in the first section of the test system represented in Fig. 5. One of the results of the application of the proposed LSE using voltages and currents signals recorded at node 650 are shown in Fig. 6. One can notice that all estimated parameters pass through an abrupt change when the HIF occurs. Before the inception of HIF, equation (14) has not a defined solution because matrix **X** is almost always singular. This characteristic shows that the proposed formulation can also be used to detect the HIF occurrence. However, it should be clear that no further studies on the distinguishing between such faults and other switching phenomena where made.

B. *HIF at section 1: global behavior of the linear LSE*

The proposed approach produces various HIF distances and parameters estimations, as explained in subsection *C* of the section III and exemplified in Fig. 6. In order to obtain unique parameters estimation, an average calculation operation was performed using an estimation set. As observed in Fig. 6, all estimations tend to stabilize when the moving windows (see J1 and J2 in Fig. 4) are completely filled with samples of the fault period. In view of this characteristic, the average was calculated using results within one cycle after 1.5 cycles of

presented in Table I, applied in ten distances along the considered section I. Each fault occurrence was selected at three time instants corresponding with the maximum positive, zero crossing and maximum negative of the faulted-phase voltage. These inception angles were respectively named as 0°, 90° and 180°. Results of the distance estimations are presented in Fig. 7 and results of the HIF parameters estimation are presented in Fig. 8. These figures present the average value of the estimation errors.

Fig. 7 presents an important characteristic, which is that the proposed approach has not shown an appreciable effect in

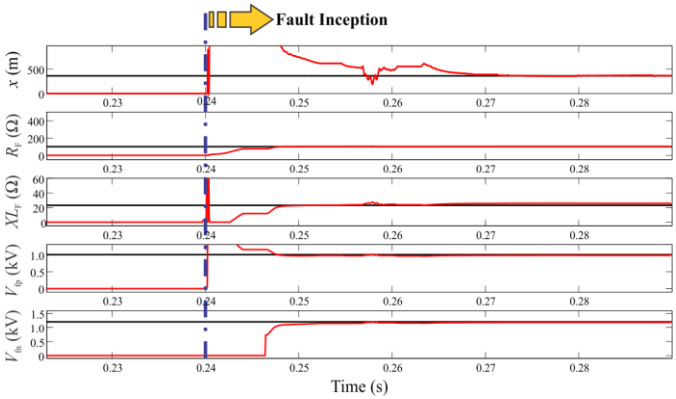

Fig. 6. Results of the proposed implementation of the LSE to estimate the HIF parameters. The simulated HIF is the number 4 (Table I) at 360 m from the substation (node 650). True values are shown in bold horizontal lines.

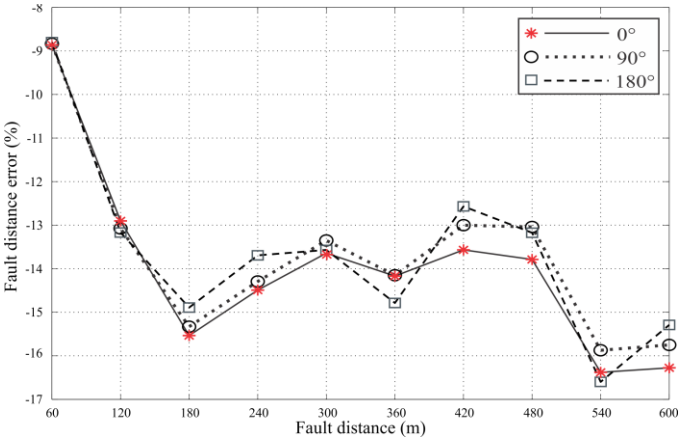

Fig. 7. Distance estimation perceptual error of the linear least squares estimator approach. Mean value.

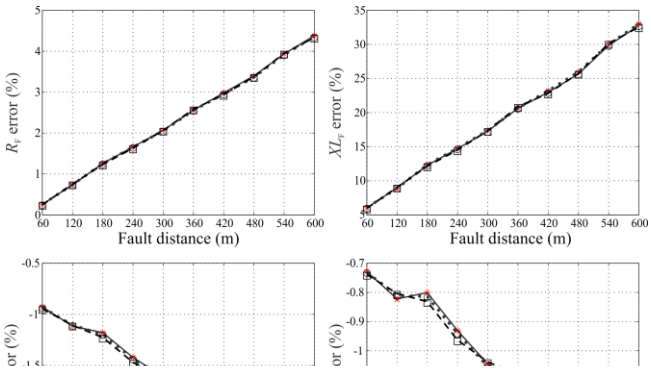

Fig. 8. HIF parameters estimation perceptual error of the linear least squares estimator approach. Mean value.

relation to the fault inception angle. The same can be said regarding to the HIF parameters estimation, as presented in Fig. 8.

The average of the distance estimation error presented in Fig. 7 maintains a negative trend, showing that the proposed method tends to under-estimate the fault distance. The error also tends to increase with the fault distance.

As shown in Fig. 8, the average estimations of R_F, V_{Fp} and V_{Fn} are significantly better than the average estimation of distance. In addition, Fig. 8 also shows that the average estimation errors present a slight increase with the fault distance. The average estimation error of L_F is not as good as the others HIF parameters and the increase of errors in function of the fault distance are more significant.

One should note that the considered faults present a nonlinear behavior. Some produce fault currents less than 10 % of the actual load current. A classical fault location method that considers the fault as a pure resistance will not produce results at all. Despite of the obtained errors on fault distance estimation, the proposed approach generates most useful estimates.

C. *HIF at section 1: consideration of line capacitance*

Results obtained with the linear LSE and presented in the

This article has been accepted for publication in a future issue of this journal, but has not been fully edited. Content may change prior to final publication. Citation information: DOI 10.1109/TPWRD.2015.2507541, IEEE Transactions on Power Delivery

previous subsection indicate that the system of equations shown in (15) presents a poorly-conditioned behavior regarding to the estimation of x and L_F. In the linear approach the line capacitance was neglected. Therefore, the proposal of the present subsection is to evaluate if the consideration of the line capacitance can produce a significant improvement of results. This is done by applying the approach presented in the subsection *D* of the section III.

Results are presented in Fig. 9 and Fig. 10, in the same way as for the linear LSE. The behavior of the NLLSE was very similar to those obtained with the linear approach. This results shows that the consideration of the line capacitance does not affect significantly the results in the considered test system.

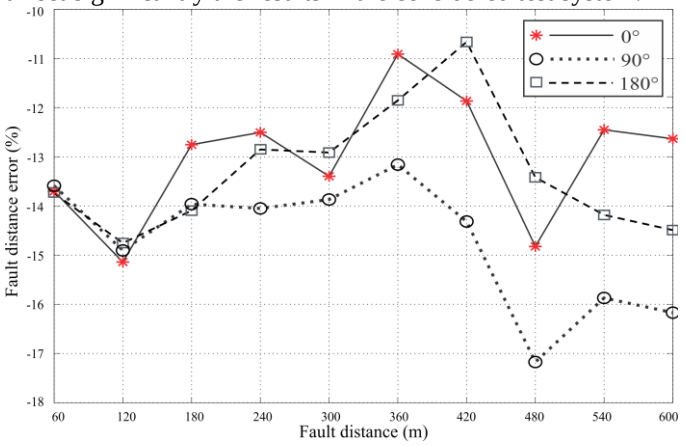

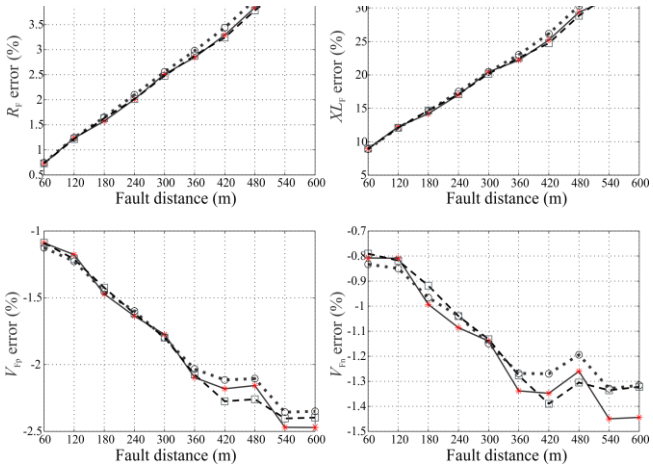

Fig. 10. HIF parameters estimation perceptual error of the nonlinear least squares estimator approach. Mean value.

D. Comparative analysis

This subsection presents a simple comparative analysis in order to highlight the contribution that the present work makes to the state of the art. Hence, the proposed approach is compared with [3]. Two fault scenarios are analyzed.

In the first case, a fault composed only by an arc and an arc resistance is simulated. This is equivalent to the fault model considered in [3] and means that $V_{Fp} = V_{Fn}$ and $L_F = 0$. The R_F parameter was set 20 Ω and the fault distance at 300 m from the bus number 650 of Fig. 5. Test results of the fault distance estimation are presented in Fig. 11. In this case, both methods presented a reasonable estimation of the fault distance. As the lines of the test system are unbalanced, the method proposed in [3] presents a slightly worse estimative. This is true because [3] is conceived using an symmetrical components approach, assuming a balanced system.

In the second case, the fault was set with V_{Fp} = 700 V, V_{Fn} = 1000 V, L_F = 0.0265 H and R_F = 20 Ω. The comparative test results of the fault distance estimation are presented in Fig. 12. In this case, the method presented in [3] does not present an accurate estimation of the fault distance. On the other hand, the proposed approach presents a good estimation in this case. Comparative tests considering fault parameters estimation were not included since [3] does not provide such.

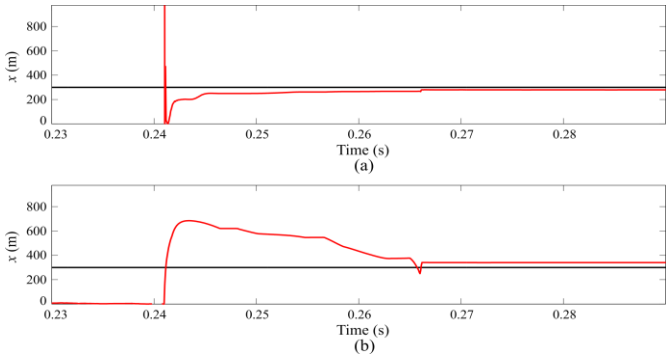

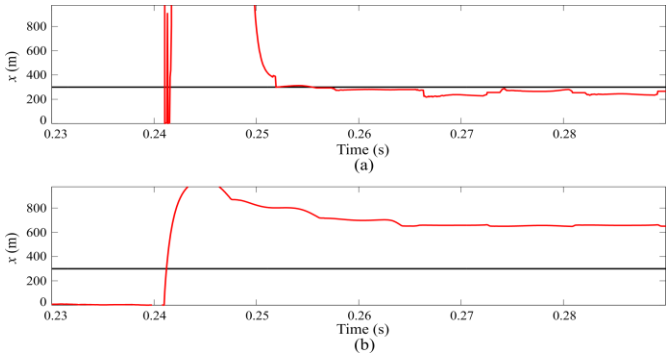

Fig. 12. Results of fault distance estimation using: (a) the proposed approach and; (b) approach presented in [3]. The fault is at 300 m from the substation (node 650), value showed in bold horizontal lines. The HIF parameters are R_F = 20 Ω, L_F = 0.0265 H, V_{Fp} = 700 V, V_{Fn} = 1000 V.

V. Conclusions

In this paper, a HIF location analytical methodology is proposed. The method uses a parameter estimation based approach for fault distance and parameters calculation. In the proposed formulation, only one terminal voltage and current signals are used and the fault location and parameters can be estimated within the first cycles after the fault inception. The technique allows consideration or not of line capacitance. If line capacitance is not considered, a linear set of equations is solved with a LSE based approach. If line capacitance is

considered, a nonlinear set of equation must be solved. For such, the proposed method is implemented in two steps. Firstly, the line capacitance is neglected and the LSE is calculated with a moving window on the signals, resulting in parameter estimation for each sample. In turn, as estimated parameters pass through an abrupt change at the fault inception instant, the proposed approach can also be used to detect the HIF occurrence. The second step was developed in order to consider the line capacitance. It consists on an iterative search technique to estimate the parameters that minimize a residual function. This is carried out with the values estimated in the linear LSE as a starting point. Test results on the study system indicate that the consideration of line capacitance resulted in similar accuracy.

A comparative analysis was made with a state-of-the-art method. Results show that when a more complete HIF model is considered, the state-of-the-art method cannot give an accurate estimation of the fault distance. On the other hand, the proposed approach gives a more accurate estimation of the fault distance providing as well the fault parameters estimation.

The analytical formulation presented in this work considers a HIF model in equation derivation. As a result, this allows the location of the fault using one terminal signals, which clearly represents a contribution to the state of the art. In view of the test results, the method is insensitive to the fault inception instant.

monitoring devices can be conceived to monitor different branches of the distribution system. The combination of this scheme with the proposed HIF location approach would considerably increase the reliability and accuracy of the fault detection and location.

REFERENCES

[1] IEEE Power System Relaying Committee, "High Impedance Fault Detection Technology," 1996.

[2] A. E. Emanuel, D. Cyganski, J. A. Orr, S. Shiller, and E. M. Gulachenski, "High impedance fault arcing on sandy soil in 15 kV distribution feeders: contributions to the evaluation of the low frequency spectrum," *IEEE Trans. Power Deliv.*, vol. 5, no. 2, pp. 676–686, Apr. 1990.

[3] M. B. Djurić, Z. M. Radojević, and V. V. Terzija, "Digital signal processing algorithm for arcing faults detection and fault distance calculation on transmission lines," *Int. J. Electr. Power Energy Syst.*, vol. 19, no. 3, pp. 165–170, Mar. 1997.

[4] M. M. Alamuti, H. Nouri, R. M. Ciric, and V. Terzija, "Intermittent fault location in distribution feeders," *IEEE Trans. Power Deliv.*, vol. 27, no. 1, pp. 96–103, 2012.

[5] S. Kulkarni, S. Santoso, and T. a. Short, "Incipient fault location algorithm for underground cables," *IEEE Trans. Smart Grid*, vol. 5, no. 3, pp. 1165–1174, 2014.

[6] A. F. Sultan, D. J. Fedirchuk, and G. W. Swift, "Detecting Arcing downed-wires using fault current flicker and half-cycle asymmetry," *IEEE Trans. Power Deliv.*, vol. 9, no. 1, pp. 461–470, 1994.

[7] Z. M. Radojević, V. V. Terzija, and M. B. Djurić, "Numerical algorithm for overhead lines arcing faults detection and distance and directional protection," *IEEE Trans. Power Deliv.*, vol. 15, no. 1, pp. 31–37, 2000.

[8] F. M. Uriarte and V. Centeno, "High-impedance fault detection and localization in distribution feeders with microprocessor based devices," *Proc. 37th Annu. North Am. Power Symp. 2005.*, pp. 219–224, 2005.

[9] L. Garcia-Santander, P. Bastard, M. Petit, I. Gal, E. Lopez, and H. Opazo, "Down-conductor fault detection and location via a voltage based method for radial distribution networks," *IEE Proc. - Gener. Transm. Distrib.*, vol. 152, no. 2, pp. 180–184, 2005.

[10] N. I. Elkalashy, M. Lehtonen, H. a. Darwish, A. M. I. Taalab, and M. a. Izzularab, "DWT-based detection and transient power direction-based location of high-impedance faults due to leaning trees in unearthed MV networks," *IEEE Trans. Power Deliv.*, vol. 23, no. 1, pp. 94–101, 2008.

[11] S. Gautam and Brahma, "Detection of High Impedance Fault in Power Distribution Systems Using Mathematical Morphology," *IEEE Trans. Power Syst.*, vol. 28, no. 2, pp. 1226–1234, May 2013.

[12] A. S. Bretas, M. Moreto, R. H. Salim, and L. O. Pires, "A Novel High Impedance Fault Location for Distribution Systems Considering Distributed Generation," in *Transmission Distribution Conference and Exposition: Latin America, 2006. TDC '06. IEEE/PES*, 2006, pp. 1–6.

[13] A. H. A. Bakar, M. S. Ali, C. Tan, H. Mokhlis, H. Arof, and H. A. Illias, "High impedance fault location in 11kV underground distribution systems using wavelet transforms," *Int. J. Electr. Power Energy Syst.*, vol. 55, pp. 723–730, Feb. 2014.

[14] D. S. Gazzana, G. D. Ferreira, a. S. Bretas, a. L. Bettiol, a. Carniato, L. F. N. Passos, a. H. Ferreira, and J. E. M. Silva, "An integrated technique for fault location and section identification in distribution systems," *Electr. Power Syst. Res.*, vol. 115, pp. 65–73, Oct. 2014.

[15] N. Zamanan and J. Sykulski, "The evolution of high impedance fault modeling," in *2014 16th International Conference on Harmonics and Quality of Power (ICHQP)*, 2014, pp. 77–81.

[16] M. R. M. Castillo, J. B. a London, N. G. Bretas, S. Lefebvre, J. Prévost, and B. Lambert, "Offline detection, identification, and correction of branch parameter errors based on several measurement snapshots," *IEEE Trans. Power Syst.*, vol. 26, no. 2, pp. 870–877, 2011.

[17] M. Ghazizadeh-Ahsaee, "Accurate NHIF locator utilizing two-end unsynchronized measurements," *IEEE Trans. Power Deliv.*, vol. 28, no. 1, pp. 419–426, 2013.

[18] R. H. Salim, K. C. O. Salim, and A. S. Bretas, "Further improvements [illegible] *Insul.*, vol. 14, no. 2, pp. 375–383, Apr. 2007.

[20] W. C. dos Santos, B. A. de Souza, N. S. D. Brito, F. B. Costa, and M. R. C. Paes, "High Impedance Faults: From Field Tests to Modeling," *J. Control. Autom. Electr. Syst.*, vol. 24, no. 6, pp. 885–896, Sep. 2013.

[21] L. A. Aguirre, *Introdução à Identificação de Sistemas: técnicas lineares e não-lineares aplicadas a sistemas reais*, 3th. ed. Belo Horizonte: Editora UFMG, 2007.

[22] D. Luenberger and Y. Ye, *Linear and Nonlinear Programming*, 3th ed. Boston, MA: Springer US, 2008.

[23] W. H. Kersting, "Radial distribution test feeders," *IEEE Trans. Power Syst.*, vol. 6, no.3, pp. 975-985, 1991.

Leonardo Ulises Iurinic (S´11) received the BSc degree in electromechanical engineering from the National University of Missiones (UNaM), Argentina in 2009, and the MSc degree in electrical engineering from the Federal University of Rio Grande do Sul (UFRGS), Brazil in 2012. He is currently pursuing the PhD degree in electrical engineering at UFRGS.

A. R. Herrera-Orozco received the BSc and MSc degree in Electrical Engineering from Technological University of Pereira (UTP), Colombia, in 2010 and 2013, respectively. He is currently pursuing the PhD degree in Electrical Engineering from the Federal University of Rio Grande do Sul.

Renato Gonçalves Ferraz (M'14) received the BSc, MSc, and PhD degrees in electrical engineering from the Federal University of Rio Grande do Sul, Brazil, in 2005, 2010, and 2014, respectively. He is currently an Assistant Professor at the University of Caxias do Sul, Brazil.

Arturo Suman Bretas (M´99) (SM´12) received the BSc and MSc degrees in Electrical Engineering from the University of São Paulo, Brazil in 1995 and 1998 respectively. At Virginia Tech, in 2001, he received his PhD degree. He is currently a Professor of the Electrical and Computer Engineering Department at the University of Florida.